Neutron scattering study on the structure-property relationship of radiation-grafted proton exchange membranes

Yue Zhao[1*], *Kimio* Yoshimura[1], *Akihiro* Hiroki[1], *Aurel* Radulescu[2], and *Yasunari* Maekawa[1]

[1]Department of Advanced Functional Materials Research, Takasaki Institute of Advanced Quantum Science, National Institutes for Quantum Science and Technology (QST), Watanuki-machi 1233, Takasaki, Gunma, 370-1292, Japan
[2]Forschungszentrum Jülich GmbH, Jülich Centre for Neutron Science @ MLZ, Lichtenbergstraße 1, D-85747 Garching, Germany

Abstract. The partial scattering function (PSF) analysis through the contrast variation small-angle neutron scattering technique was used to determine the exact structure of the hydrated radiation-grafted proton-exchange membranes, made of poly(styrene sulfonic acid)-grafted poly(ethylene-co-tetrafluoroethylene) (ETFE-g-PSSA) with a high ion exchange capacity of 2.5 mmol/g. The membrane was treated as a three-component system composed of ETFE base polymer, PSSA graft polymer, and absorbed water. The analysis on PSF self-terms gave the exact structure of individual components and that on PSF cross-terms explored the correlation between two components to establish their locations. The characterization was performed in multiple length scales, and the mechanistic insights into membrane conductivity and structure correlations were provided.

1 Introduction

Radiation-grafted proton exchange membranes (PEMs), made of poly(styrenesulfonic acid)-grafted poly(ethylene-co-tetrafluoroethylene) (ETFE-g-PSSA), are promising alternatives to Nafion® membranes for electrochemical applications such as electrodialysis and fuel cells. They offer the advantages of a potentially low-cost fabrication technique, and the adaptability of both improving membrane ionic conductivity by PSSA graft polymers and maintaining the excellent mechanical/thermal properties of ETFE base polymer [1-3]. To the current stage of research, challenges remained to overcome are the relatively low proton conductivity of ETFE-g-PSSA under reduced relative humidity and long-term stability, which need thorough understanding of structure-property relationships [1-9].

It is known that in hydrated ETFE-g-PSSA PEMs, the sulfonic acid (SA, -SO_3H) groups absorb water and form hydrophilic ionic channels that phase segregate from the hydrophobic polymer matrix. Thus, the proton conductivity is strongly controlled by the morphology and connectivity of ion channels [4-9]. As one of the most essential techniques to understand the nano-scaled structure of a hydrated material, small-angle neutron scattering (SANS) technique has been employed in the previous studies. However, the conventional scattering analysis is based on the scattering intensity profile that contains contributions of all components in the system such as the hydrophobic polymer, hydrophilic polymer, ions, and water molecules, and fails to provide the detailed structure of the individual components. This undesirable original data problem was recently solved by partial scattering function (PSF) analysis, which is the quantitative decomposition of a series of intensity profiles obtained through contrast-variation SANS (CV-SANS) experiments [10-12]. PSF analysis was applied to polymer nanocomposites in early studies [10], and recently was developed by us for Nafion and ETFE-g-PSSA PEMs with moderate ion exchange capacity (IEC) of 1.0 ~ 2.0 mmol/g [11,12].

In this article, we extended the application of this PSF analysis to determine the detailed structure of ETFE-g-PSSA PEMs with a high IEC of 2.5 mmol/g (denoted as ETFE-g-PSSA_2.5). The unique capability that PSF analysis provides to understanding structure correlations can result into new insights on the role of the polymer micro-/nano- structure and water in the emergence of the ion conduction. This in turn can help in the design of high-performing PEMs for a wide range of energy conversion applications.

2 Experimental details

2.1 Materials

The ETFE base film with a thickness of 50 μm (mass density, d_{BP} = 1.75 g/cm^3, crystallinity = 0.32) were purchased from Asahi Glass Co. Ltd, Japan. ETFE-g-PSSA_2.5 membrane with a grafting degree (GD) of 60% and an IEC of 2.5 mmol/g was prepared according to our previous report [13]. The water uptake (WU) was estimated to be ~65% at room temperature, which is defined by $WU = \frac{W_{wet}-W_{dry}}{W_{dry}} \times 100\%$, with W_{dry} and W_{wet} being the weight of the dry and water-equilibrated membrane, respectively. The conductivity of the

* Corresponding author: zhao.yue@qst.go.jp

membrane was 0.12 S/cm at 60 ºC in liquid water measured by electrochemical impedance spectroscopy.

2.2 CV-SANS measurements

CV-SANS measurements were performed on KWS-2 SANS diffractometer operated by Juelich Centre for Neutron Science (JCNS) at the neutron source Heinz Maier–Leibnitz (FRM II reactor) in Garching, Germany [14]. The incident neutron beam was monochromatized with a velocity selector to have an average wavelength (λ) of 5 Å with a wavelength resolution of 20%. Measurements were performed on ETFE-g-PSSA_2.5 PEMs equilibrated in H_2O/D_2O mixtures with eight different volume fractions of D_2O (f_{D2O}= 100, 90, 80, 70, 60, 50, 40, 0%) at room temperature. The scattering patterns were collected using a two-dimensional scintillation detector and circularly averaged to obtain scattering intensity profiles, $I(q)$s, as a function of scattering vector, q. The final $I(q)$s were corrected for the background, the electronic noise, detector sensitivity, and incoherent scattering.

3 Results and discussion

3.1 Theoretical development of PSF analysis for ETFE-g-PSSA_2.5 PEM

The ETFE-g-PSSA_2.5 PEM is partitioned into separate components of ETFE base polymer (BP, $–CH_2CH_2CF_2CF_2–$), graft polymer (GP, $–C_8H_7–SO_3H$), and water (W). The scattering length density (SLD) of each component is calculated using the chemical structure and mass density being 2.74 and 1.96 ($\times 10^{10}$ cm^{-2}) for BP (b_{BP}) and GP (b_{GP}), respectively [15]. SLD of water (b_W) varies as a function of f_{D2O} of the water mixture as

$$b_w = b_{D2O} f_{D2O} + b_{H2O}(1-f_{D2O}) \quad (1)$$

where b_{D2O} and b_{H2O} are the SLD of D_2O and H_2O being 6.34 and −0.56 ($\times 10^{10}$ cm^{-2}), respectively.

According to incompressibility assumption, $I(q)$ can be described by three PSF self-terms $S_{ii}(q)$ as follows,

$$I(q)=(b_{BP}-b_{GP})(b_{BP}-b_W)S_{BP\text{-}BP}(q)+(b_{GP}-b_{BP})(b_{GP}-b_W)S_{GP\text{-}GP}(q)+(b_W-b_{BP})(b_W-b_{GP})S_{W\text{-}W}(q) \quad (2)$$

where S_{ii} is PSF self-term of the i component (i = BP, GP and W), representing its structural information.

CV-SANS experiments are performed with m different contrast by using H_2O/D_2O mixtures, the obtained $I(q)$s are a group of linear equations of Eq (2), Thus, three PSF self-terms of $S_{BP\text{-}BP}(q)$, $S_{GP\text{-}GP}(q)$ and $S_{W\text{-}W}(q)$ on the right side of Eq. (2) can be mathematically determined through the simultaneous equations of $I(q)$ [11, 12].

The PSF cross-term S_{ij} ($i \neq j$) contains information about the interaction between the i and j components and can be deduced from S_{ii} using Eqs (3)–(5) below.

$$S_{BP\text{-}GP}=1/2(S_{W\text{-}W}-S_{BP\text{-}BP}-S_{GP\text{-}GP}) \quad (3)$$

$$S_{GP\text{-}W}=1/2(S_{BP\text{-}BP}-S_{GP\text{-}GP}-S_{W\text{-}W}) \quad (4)$$

$$S_{BP\text{-}W}=1/2(S_{GP\text{-}GP}-S_{BP\text{-}BP}-S_{W\text{-}W}) \quad (5)$$

3.2 Results of PSF analysis

$I(q)$ profiles are plotted as a function of q in Figure 1 for representative f_{D2O} in the CV-SANS measurements. They show typical scattering features in that a small-q upturn and two scattering maxima in three q-regions. In region I at q < 0.12 nm^{-1}, the small-q upturn follows a power-law relationship with an exponent of about −2.4. In Region II at 0.12 < q < 1.7 nm^{-1}, a shoulder-like scattering peak appears at q_1 ~ 0.17 nm^{-1}, corresponding to a d-spacing (=$2\pi/q_1$) ~ 36.9 nm. In Region III at q > 1.7 nm^{-1}, the second scattering peak, so-called "ionomer peak", appears at q_2 = 2.6 nm^{-1}, with a d-spacing (=$2\pi/q_2$) of 2.4 nm.

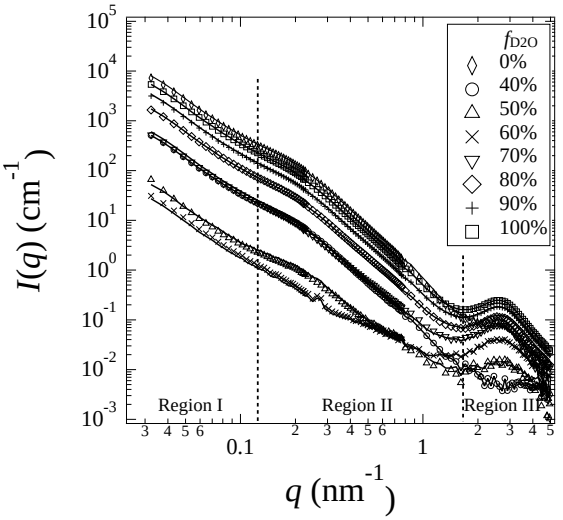

Fig. 1 Experimental scattering intensity profiles (symbols) and the reconstructed intensity profiles (solid lines) of the fully hydrated ETFE-g-PSSA_2.5 PEMs equilibrated in water mixtures of D_2O and H_2O with different ratios.

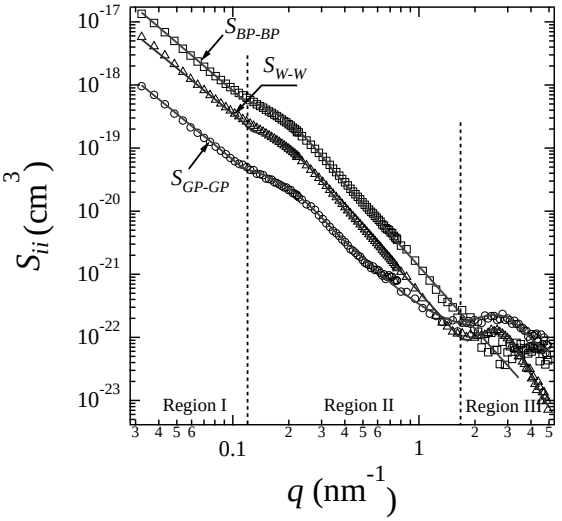

Fig. 2 PSF self-terms of the fully hydrated ETFE-g-PSSA_2.5 PEMs (symbols) and the best-fitted results (solid lines).

The self-terms of PSFs including $S_{BP–BP}$, $S_{GP–GP}$, and $S_{W–W}$ were calculated based on section 3.1 and plotted as a function of q in Figure 2. In Region I, all S_{ii} exhibit an upturn with a power-law exponent of about −2.4. In Region II, all S_{ii} shows a shoulder-like scattering maximum with a centre position close to the peak observed in $I(q)$ profiles in Figure 1. In Region III, $S_{GP–GP}$ and $S_{W–W}$ show a peak with a centre position close to

the ionomer peak, and the peak in S_{GP-GP} is broader than that in S_{W-W}. On the contrary, S_{BP-BP} in Region III is flat, revealing ETFE BP is structureless at this length scale. With these three S_{ii}, all reconstructed $I(q)$ profiles (solid lines) using Eq (2) via back-substitution are well matched to the experimental profiles (symbols) in Figure 1, evidencing the correctness of S_{ii}.

As mentioned in section 3.1, S_{ii} reflects the concrete structure of the i component, including its arrangement and phase-separated morphology in the membrane. Since S_{ii} show similar features to the previously studied ETFE-g-PSSA PEMs with an IEC of 2.0 mmol/g (denoted as ETFE-g-PSSA_2.0) [12], we reasonably propose the same fitting functions here to interpret S_{ii}: Mass fractal (MF) structure model to describe the small-q upturn in Region I, the unified Guinier-exponential function (GE model) to fit the shoulder peak in Region II, and Teubner-Strey (TS) model to describe the local structure in Region III. However, it should be noted that the scattering origin for the two membranes ETFE-g-PSSA_2.0 and ETFE-g-PSSA_2.5 are different. It is the aggregation of individual GP nanodomains in the hydrophobic BP matrix that makes the structure pattern of ETFE-g-PSSA_2.0, while the structure of the ETFE-g-PSSA_2.5 is originated from the aggregation of hydrophobic BP nanodomains in the GP matrix. This difference is evidenced by taking account of the volume fraction of BP in the hydrated PEMs, ϕ_{BP},

$$\phi_{BP} = \frac{\frac{1}{d_{BP}}}{\frac{1}{d_{BP}}+\frac{GD/100}{d_{GP}}+\frac{WU/100(1+GD/100)}{d_w}} \quad (6)$$

where d_x (x=BP, GP and W) is the mass density of x being approximately 0.55 and 0.3 for ETFE-g-PSSA_2.0 and ETFE-g-PSSA_2.5, respectively.

Thus, S_{ii} of ETFE-g-PSSA_2.5 is the sum of the three models given by

$$S_{ii}(q)=C_1S_{MF}(q)+C_2S_{GE}(q)+C_3S_{TS}(q)+C_B \quad (7)$$

where C_1, C_2, and C_3 are the fitting constants, and C_B is the constant background. The first term $S_{MF}(q)$ is expressed as

$$S_{MF}(q) \propto \frac{\Gamma(D_f-1)}{(1+q^2\xi^2)^{(D_f-1)/2}} \times \frac{\sin[(D_f-1)\tan^{-1}(q\xi)]}{q\xi} \quad (8)$$

which is the MF function with the gamma function (Γ), MF dimension (D_f), and the upper cutoff length of the MF structure (ξ) being roughly estimated as ~150 nm according to the previous report using the Ultra-SAXS method [13]. The second term, $S_{GE}(q)$, is proposed to describe the structure of irregularly shaped individual BP nano-domains as expressed below.

$$S_{GE}(q) \propto \exp\left(\frac{-q^2R_g{}^2}{3}\right) + B\left\{\frac{[\mathrm{erf}\left(\frac{kqR_g}{\sqrt{6}}\right)]^3}{q}\right\}^P \quad (9)$$

where R_g is the radius of gyration of individual BP particle, erf(x) is the error function of x, k is an empirical constant equal to 1.06. P ($3 < P < 4$) describes the particle's surface fractal dimension, and B is a constant prefactor. The third term, $S_{TS}(q)$, is the scattering function of the TS model describing bicontinuous-shaped domains with short-range order as below:

$$S_{TS}(q) \propto \frac{8\pi d^4}{\varepsilon[16\pi^4+8d^2\pi^2(\varepsilon^{-2}-q^2)+d^4(\varepsilon^{-2}+q^2)^2]} \quad (10)$$

where d is the mean separation distance between two domains determined from the peak position, q_m ($d = 2\pi/q_m$), and ε is considered as the dispersion of d (inversely proportional to the peak width). A smaller ε resulted from a broader peak indicates a more disordered bicontinuous structure. The best-fitted curves obtained using Eq. (7) are shown together with S_{ii} in Figure 2, and all the fitting parameters are listed in Table 1.

Table 1. Fitting parameters in Eq (7).

Models	MF		GE		TS	
S_{ii}	ξ(nm)	D_f	R_g(nm)	P	d(nm)	ε(nm)
S_{BP-BP}	150	2.4	10.0	3.3	-	-
S_{GP-GP}	150	2.4	10.0	3.1	2.2	0.9
S_{W-W}	150	2.4	10.0	3.1	2.3	1.2

The PSF cross-terms S_{ij} ($i \neq j$) through Eqs.(3)–(5) reflect cross-correlation between the components i and j. The positive and negative sign of S_{ij} reveals the interaction force between i and j, denoting attractive and repulsive interactions, respectively. The cross-terms of PSFs as a function of q are shown in Figure 3. S_{BP-GP} and S_{BP-W} are always negative, whereas the sign of S_{GP-W} is opposite at q lower and higher than 1.5 nm^{-1} as shown in the inset, respectively.

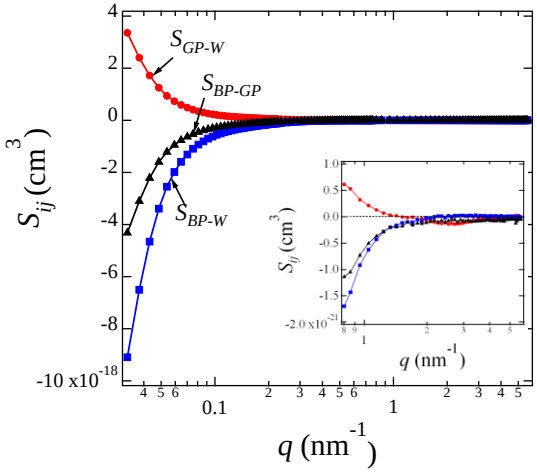

Fig. 3 PSF cross-terms of the fully hydrated ETFE-g-PSSA_2.5 PEMs. Enlarged plots at q > 1 nm^{-1} in the inset.

3.3 Visualization of three-component domains in the hydrated ETFE-g-PSSA_2.5 PEM

3.3.1 Large scale structure

The MF model describes a structure consists of self-similar polymer particles within a spatial range. Based on the analysis of S_{ii} in Region I, the schematic picture of the large-scale structure is shown in Figure 4 (a). Note that BP hydrophobic domains are clearly phase-separated from hydrophilic domains made of GP and water, as evidenced by the repulsive interactions suggested by the negative sign of S_{BP-GP} and S_{BP-W}. All

components show a similar mass fractal structure with a dimension of D_f = 2.4, indicating a dense packing of BP nano-domains in space, close to percolating networks. Instead, GP and water domains form the compensative matrix according to Babinet's principle, therefore, S_{GP-GP} and S_{W-W} shows the same MF structure feature as S_{BP-BP} does. In addition, the positive S_{GP-W} indicates that water is closely attached to GP due to the hydrophilic nature of SA groups. Therefore, water domains coordinatively move with GP domains.

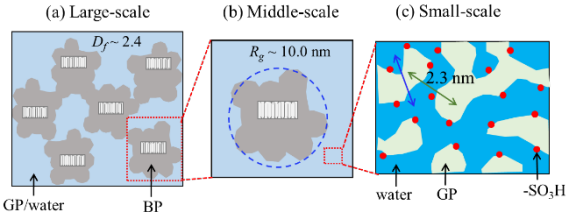

Fig. 4 Schematic of the hierarchical structure of the individual components in the fully hydrated ETFE-g-PSSA_2.5 PEMs at (a) large-scale; (b) middle-scale; and (c) small-scale.

3.3.2 Middle scale structure

The GE model analysis in Region II shows all domains have a characteristic R_g of ~10.0 nm, which is the average size of the individual building blocks for each component to form the MF structure in Region I. Since GP and water domains coordinatively move, we reasonably conclude that BP nano-domains with a size of R_g = 10 nm are distributed in the homogeneous matrix of GP and water. The power-law relationship in the high-q-regime in Region II allows for the estimation of P, which is an indicative of the surface roughness of the domain. P is in the range of 3.1-3.3, smaller than the typical sharp Porod surface (P = 4), indicating a rough domain surface. Based on the above discussion, a schematic of the structure in Region II is shown in Figure 4(b).

3.3.3 Small scale structure

The detailed local structure in a GP/water domain is explained by TS model analysis of S_{GP-GP} and S_{W-W} that shows both components have bicontinuous-like structure with similar d value (2.2–2.3 nm) as schematically shown in Figure 4(c). S_{GP-W} is negative in this region with a molecular length level < 3.7 nm (q > 1.7 nm^{-1}), indicating a repulsion between GP and water probably due to the strong repulsive force between PS polymer and water. This result is in good agreement with what we observed in ETFE-g-PSSA_2.0 PEM, and much different from Nafion membrane where the interaction between polymer side chain and water are positive. This considerable difference results in the low swelling of ETFE-g-PSSA_2.5 PEM but high conductivity under low relative humidity conditions, as compared to Nafion.

The detailed structure evolution of ETFE-g-PSSA_2.5 at multiple length scales illustrates the power of PSF analysis to gain insight into structure-property relationships in disordered and bi-continuous systems.

4 Conclusions

We applied PSF analysis to gain quantitative knowledge of the role of each component in the entire structure of fully hydrated radiation-grafted ETFE-g-PSSA_2.5 PEMs by CV-SANS experiments. Our results suggested three-component domains consisting of ETFE base polymer, PSSA graft polymers and water. PSF self-terms analysis revealed the detailed structure of each component, whereas the cross-terms gave the correlation between two components, leading to the location determination of the components. The entire structure patterns of the hydrated PEM were constructed in Figure 4. PSF analysis provides mechanistic insights concerning structural correlations over a range of length scales, from micro-/nano-meter to molecular scale, which offers the structural guidelines in the design of high-performing PEMs for a wide range of energy conversion applications.

References

1. M. M. Nasef, Chem. Rev., **114**, 12278 (2014).
2. J. A. Horsfall, K. V. Lovell, Fuel Cells, **1**, 186 (2001).
3. A. Aricò, V. Baglio, P. Creti, A. Di blasi, V. Antonucci, J. Brunea, A. Chapotot, A. Bozzi, J. Schoemans, J. Power Sources, 123, 107 (2003).
4. S. A. Gürsel, L. Gubler, B. Gupta, G. G. Scherer, in Fuel Cells I (Springer, Berlin, Heidelberg, 2008).
5. S. Balog et al., Macromolecular Chemistry and Physics 211, 635-64 (2010).
6. K. Mortensen et al., Journal of Polymer Science Part B-Polymer Physics 46, 1660 (2008).
7. V. Sproll et al., Macromolecules 49, 4253 (2016).
8. S. Balog et al., Polymer 53, 175 (2012).
9. S. Balog et al., Journal of membrane science 383, 50 (2011).
10. H. Endo, D. Schwahn, H. Colfen, J. Chem. Phys. **120**, 9410 (2004).
11. Y. Zhao, K. Yoshimura, T. Motegi, A. Hiroki, A. Radulescu, Y. Maekawa, Macromolecules, **54**, 4128 (2021).
12. Y. Zhao, K. Yoshimura, S. Sawada, T. Motegi, A. Hiroki, A. Radulescu, Y. Maekawa, Macromolecules, **55**, 7100 (2022).
13. T. D. Tap, S. Sawada, S. Hasegawa, K. Yoshimura, Y. Oba, M. Ohnuma, Y. Katsumura, Y. Maekawa, Macromolecules, **47**, 2373 (2014).
14. A. Radulescu, V. Pipich, H. Frielinghaus, M. S. Appavou, Journal of Physics: Conference Series, **351**, 012026 (2012).
15. R. J. Roe, Methods of X-ray and neutron scattering in polymer science (Oxford Uni. Press, New York, 2000).